Conditional Vascular Cell Adhesion Molecule 1 Deletion in Mice: Impaired Lymphocyte Migration to Bone Marrow

By Pandelakis A. Koni,* Sunil K. Joshi,* Ulla-Angela Temann,‡ Dian Olson,‖ Linda Burkly,‖ and Richard A. Flavell‡§

*From the *Molecular Immunology Program, Institute of Molecular Medicine and Genetics, and Department of Medicine, Medical College of Georgia, Augusta, Georgia 30912; the ‡Section of Immunobiology and §Howard Hughes Medical Institute, Yale University School of Medicine, New Haven, Connecticut 06520; and ‖Biogen Incorporated, Boston, Massachusetts 02142*

Abstract

We generated vascular cell adhesion molecule (VCAM)-1 "knock-in" mice and Cre recombinase transgenic mice to delete the VCAM-1 gene (*vcam-1*) in whole mice, thereby overcoming the embryonic lethality seen with conventional *vcam-1*–deficient mice. *vcam-1* knock-in mice expressed normal levels of VCAM-1 but showed loss of VCAM-1 on endothelial and hematopoietic cells when interbred with a "TIE2Cre" transgene. Analysis of peripheral blood from conditional *vcam-1*–deficient mice revealed mild leukocytosis, including elevated immature B cell numbers. Conversely, the bone marrow (BM) had reduced immature B cell numbers, but normal numbers of pro-B cells. *vcam-1*–deficient mice also had reduced mature IgD^+ B and T cells in BM and a greatly reduced capacity to support short-term migration of transferred B cells, $CD4^+$ T cells, $CD8^+$ T cells, and preactivated $CD4^+$ T cells to the BM. Thus, we report an until now unappreciated dominant role for VCAM-1 in lymphocyte homing to BM.

Key words: VCAM-1 • Cre recombinase • knockout mice • bone marrow • lymphocyte migration

Introduction

Leukocyte trafficking is a dynamic orchestration of molecular cues. Numerous molecules participate in one or more steps in an integrated multistep process of leukocyte rolling on the blood vessel wall, followed by "activation," firm adherence, and transmigration into tissue (1–3). One of the players in this scenario is vascular cell adhesion molecule (VCAM)[1]-1, which mediates both rolling on endothelial cells (ECs) and firm adherence (4–7). VCAM-1 was originally identified on the surface of activated human umbilical vein ECs as a mediator of adhesion with melanoma cells and lymphocytes (8–10). VCAM-1 expression can be induced by numerous factors, including TNF-α, IL-1, IL-4, IL-13, and intercellular adhesion molecule (ICAM)-1 cross-linking (8–14). The ability of VCAM-1 to facilitate leukocyte adherence to ECs is thought to be a critical factor in the initiation and/or perpetuation of inflammation and autoimmunity. Upregulated VCAM-1 expression on ECs is associated with several diseases including multiple sclerosis, allograft rejection, atherogenesis, rheumatoid arthritis, appendicitis, dermatitis, and inflammatory bowel disease (15–23).

Besides inducible expression on ECs, VCAM-1 is expressed on peripheral LN (PLN) and mesenteric LN (MLN) high endothelial venules (HEVs; reference 24), bone marrow (BM) stromal cells (25), BM microvasculature (7, 26, 27), thymic epithelial cells (28), spleen stromal cells (29, 30), and spleen red pulp macrophages and dendritic cells (DCs) (31, 32). Although not normally expressed by T cells, VCAM-1 is reportedly expressed by thymocytes and T cells undergoing apoptosis (33). VCAM-1 on HEVs has an apparently redundant role in lymphocyte migration to LNs (24), whereas VCAM-1 on BM microvessels has an overlapping role with selectins in hematopoietic progenitor cell recruitment into the BM compartment (7, 34). VCAM-1 on BM stromal cells might have a role in B cell development. Anti–VCAM-1 antibody greatly reduced B lymphocyte formation in long-term BM

Address correspondence to Pandelakis A. Koni, Rm. CA2007, Institute of Molecular Medicine and Genetics, Medical College of Georgia, 1120 15 St., Augusta, GA 30912. Phone: 706-721-6897; Fax: 706-721-7959; E-mail: lak@immag.mcg.edu

[1]*Abbreviations used in this paper:* BM, bone marrow; CG, chicken γ-globulin; CMFDA, 5-chloromethylfluorescein diacetate; DC, dendritic cell; EC, endothelial cell; ES, embryonic stem; FDC, follicular dendritic cell; GC, germinal center; HEV, high endothelial venule; ICAM, intercellular adhesion molecule; MLN, mesenteric LN; NP, 4-hydroxy-3-nitrophenyl; PLN, peripheral LN; PNA, peanut agglutinin; VCAM, vascular cell adhesion molecule; VLA, very late antigen.

 J. Exp. Med. © The Rockefeller University Press • 0022-1007/2001/03/741/13 $5.00
Volume 193, Number 6, March 19, 2001 741–753
http://www.jem.org/cgi/content/full/193/6/741

cultures (25). This is seemingly in contrast to studies with BM stromal cell clones from VCAM-1 null mice, where long-term maintenance and proliferation of clonable pre-B cells, cobblestone formation, and differentiation to IgM-secreting mature B cells were equally possible on VCAM-1$^+$ and VCAM-1$^-$ BM stromal cells (35). Studies of α_4 integrin–deficient hematopoietic progenitors in chimeric mice revealed a defect in α_4 integrin–deficient B cell development at the pre-B cell stage (36), reinforcing the principle of a role in B cell development for VCAM-1 or some other α_4 integrin receptor. That is, the heterodimeric integrins $\alpha_4\beta_1$ (very late antigen [VLA]-4) and $\alpha_4\beta_7$ bind VCAM-1, but VLA-4 (the principal VCAM-1 ligand) also binds fibronectin and itself via homotypic aggregation (37–44).

Recent studies also suggest that VCAM-1 might be more promiscuous than at first appreciated, in that $\alpha_D\beta_2$ (expressed by a variety of leukocytes) and $\alpha_9\beta_1$ (expressed by neutrophils) also bind to VCAM-1 (45–47). Thus, VCAM-1 may have roles besides the potential roles revealed by α_4 integrin–deficient hematopoietic progenitors. Attempts by others to further investigate the roles of VCAM-1 using genetically deficient mice met with limited success because *vcam-1* deficiency caused embryonic lethality in two independent studies (31, 48), although a few VCAM-1 null mice did survive embryonic lethality (31, 35). This hurdle has been overcome here by the generation of *vcam-1* "knock-in" mice and "TIE2Cre" Cre recombinase transgenic mice. *vcam-1* knock-in mice express normal levels of VCAM-1 but allow deletion of the *vcam-1* gene promoter and first exon, using the Cre recombinase/*loxP* system. When intercrossed with TIE2Cre transgenes, *vcam-1* knock-in mice showed virtually complete loss of VCAM-1 on ECs and hematopoietic cells. These semiregulated *vcam-1*–deficient mice had reduced immature B cells and mature lymphocytes in BM, and a greatly reduced capacity to recruit B cells and T cells to BM in short-term migration assays.

Materials and Methods

Generation of VCAM-1 Knock-in Mice. The VCAM-1 gene (*vcam-1*) was isolated from a λ Fix II 129/Ola library. The targeted region spans a 7-kb region between an upstream BamHI site and the 3′ end of the pGEM4 clone (see Fig. 1). This 3′ end does not include the BamHI site, which is expected to be slightly further downstream in *vcam-1* (49–51). The 7-kb targeted region was subcloned into pBluescript II (Stratagene) as two separate halves: an upstream BamHI-EcoRI region and a downstream EcoRI-SalI region (using the pGEM4 SalI site at the 3′ end). A HindIII fragment containing a herpes simplex virus thymidine kinase (HSV-tk) gene cassette (52) was inserted into the BamHI site of the upstream *vcam-1* fragment clone after Klenow end-filling. This modified upstream *vcam-1* clone constituted the left arm of the targeting construct.

The BamHI site in the downstream *vcam-1* clone (in the pBluescript II polylinker) was eliminated by Klenow end-filling and religation. A *loxP* site oligonucleotide duplex was designed to incorporate a BamHI site and EcoRI overhangs, but with a true EcoRI site only at the 5′ end next to the BamHI site (sense strand: 5′-phosphate-AATTCGGATCCATAACTTCGTATAGCATACATTATACGAAGTTATGC; antisense strand: 5′-phosphate-AATTGCATAACTTCGTATAATGTATGCTATACGAAGTTATGGATCCG). The two oligonucleotides were annealed together and ligated into the EcoRI site of the modified downstream *vcam-1* clone. The reappearance of a BamHI site was used to screen for positive clones. Clones that had the desired *loxP* site orientation and correct sequence were identified by sequencing with the pBluescript II reverse primer. The desired orientation of the *loxP* was that which placed the newly introduced BamHI site and the one remaining EcoRI site at the 5′ end of the *loxP* sequence and *vcam-1* fragment rather than between the two.

An XhoI site was then introduced into the HindIII site in intron 1 of the modified downstream *vcam-1* clone by partial HindIII digestion and ligation with an oligonucleotide duplex bearing HindIII site overhangs and an XhoI site. Clones with an XhoI site inserted into the desired HindIII site in intron 1 without loss of the small HindIII intron 1 fragment (see Fig. 1) were identified by digestion with BamHI, HindIII, XhoI, and combinations thereof.

A *loxP*-flanked neomycin resistance cassette was then inserted into the newly introduced XhoI site of the modified upstream *vcam-1* clone as an XhoI-SalI fragment from pLox2neopA (see below). The desired orientation of the insert (see Fig. 1) was identified by digestion with BamHI, EcoRI, XhoI, and combinations thereof. This modified downstream *vcam-1* clone constituted the right arm of the targeting construct. The construct pLox2neopA (Koni, P., and R. Flavell, unpublished results) contains a neomycin resistance cassette from pMC1neopA (Stratagene) flanked by *loxP* sites in pBluescript II (Stratagene). pLox2neopA was created with SalI and XhoI sites at the 5′ and 3′ ends (relative to the neomycin resistance cassette), respectively (as well as several other sites).

The left and right arms of the targeting construct were then joined by first excising the left arm, by partial digestion with EcoRI and then complete digestion at the pBluescript II polylinker NotI site. The full-length 4.5-kb left arm was then inserted into the right arm construct between the upstream polylinker NotI and EcoRI sites. Both the left and right arms of the targeting construct were therefore ~2.7 kb in size (excluding the 1.6-kb *loxP*-flanked *vcam-1* promoter/exon 1 region). The targeting vector was linearized at the 3′ SalI site and 25 μg was used to electroporate 10^7 W9.5 embryonic stem (ES) cells. ES cells were then plated onto mitomycin C–treated primary embryonic fibroblasts. Double drug selection for homologous recombinants was begun 24 h later with 2 μM gancyclovir (Syntex) and 0.3 mg/ml G418 (GIBCO BRL).

ES cell colonies and subsequent mice were screened by BamHI digest Southern blot analysis using probes A and B (see Fig. 1). Probe A was a 1.0-kb EcoRI-EcoRV fragment. Probe B was a 1.0-kb SphI-SalI fragment at the 3′ end of the genomic clone. All probes were products of ^{32}P incorporation by random priming using [^{32}P]dCTP (Amersham Pharmacia Biotech) and a Prime-It II kit (Stratagene). Homologous recombinant ES cells were injected into C57BL/6 blastocytes and chimeric males were bred to C57BL/6 females. Heterozygous targeted mice still bearing the neomycin resistance cassette in *vcam-1* intron 1 (*vcam*$^{+/neo}$) were thus derived from one out of four homologous recombinant ES cell clones and were then interbred to obtain *vcam-1*$^{neo/neo}$ mice and wild-type littermates. All mice were housed in specific pathogen-free conditions in accordance with institutional animal care and use guidelines.

To avoid any possible interference with VCAM-1 expression,

the neomycin resistance cassette was then deleted to create the *vcam-1*^{flox} allele (see Fig. 1 B for definitions). This "partial" deletion was achieved by use of the *splicer* mouse (see below).

Generation of Cre Recombinase Transgenic Mice. *Splicer* mice were generated with a transgene from pTet-Cre, which contains the Cre recombinase coding sequence from pBS185 (GIBCO BRL) cloned into the EcoRV site of pTet-Splice (GIBCO BRL) as a Klenow-blunted MluI-XhoI fragment. TIE2Cre transgenes were generated with a TIE2 kinase promoter/enhancer cassette described previously (53). The construct pSPTg.T2FXK (pg54) (a gift from Thomas Sato, Beth Israel Hospital, Boston, MA) contained the TIE2 kinase promoter and enhancer with HindIII and NotI sites between the two. These sites allowed us to directionally clone a HindIII-NotI fragment from pTet-Cre, thus introducing the Cre recombinase coding sequence, intronic donor/acceptor sequences, and polyadenylation signal sequences into pg54. This TIE2Cre transgene was then excised from the vector backbone using SalI.

All transgenic mice were generated on a (C3H × C57BL/6)F_2 background. Screening of tail DNA for Cre recombinase transgene presence was by PCR with the following primers: forward, 5′-CGATGCAACGAGTGATGAGG-3′; and reverse, 5′-CGCATAACCAGTGAAACAGC-3′. Positive founder mouse lines were then crossed with C57BL/6 mice for two generations before interbreeding with VCAM-1 knock-in mice.

Lung Challenge and Immunohistology. Mice were given an intraperitoneal injection of alum-precipitated antigen consisting of 20 μg OVA (grade V; Sigma-Aldrich) adsorbed onto 2 mg aluminum hydroxide in 0.1 ml PBS. A booster injection was given 5 d later. Control animals received precipitated alum in PBS only. 12 d after the first sensitization, mice were challenged by exposure to an aerosol of 0.5% OVA in PBS, twice for 1 h each with a 4-h interval. This was done by placing the mice in a Plexiglass chamber attached to an ultrasonic nebulizer (1–5 μm particles; DeVilbiss), with a small hole to allow continuous airflow.

Lungs were excised 2 d later, inflated with 1:3 dilution of Tissue-Tek OCT Compound (VWR Scientific) in PBS, and then frozen in OCT compound using a dry ice/methylbutane bath. Sections were cut onto silanized glass slides at 7-μm thickness and allowed to air dry for 1 h before being fixed in cold acetone for 10 min and stored at −70°C until use.

For staining, sections were rehydrated in wash buffer (0.1 M Tris-Cl, pH 7.4, 0.01% Triton X-100) for 10 min. Sections were then incubated with blocking buffer (3% BSA in wash buffer) for 30 min, and with avidin/biotin blocking kit (Vector Laboratories) for 15 min for each step. Sections were rinsed briefly in wash buffer before incubation for 1 h with biotin-conjugated anti–mouse VCAM-1 (MVCAM.A; BD PharMingen) diluted in 1% BSA/wash buffer. The sections were then washed three times for 5 min in wash buffer and incubated for 40 min with an appropriate dilution of streptavidin–alkaline phosphatase (Zymed Laboratories) in 1% BSA/wash buffer. The sections were then washed and developed using HistoMark Red staining system (KPL), counterstained with Meyer's hematoxylin, and mounted using Permount (Fisher Scientific).

ROSA26R Cre Reporter β-Galactosidase Histology. ROSA-26R reporter mice (54) were purchased from The Jackson Laboratory and maintained in our facility in accordance with institutional animal care and use guidelines. After crossing with the TIE2Cre transgene, progeny were genotyped by Cre recombinase PCR as described earlier, and by ROSA26R PCR using primers as described elsewhere (54). ROSA26R$^+$ mice were anesthetized at 6–7 wk of age with Avertin and perfused with 4% paraformaldehyde in PBS by cardiac puncture. Various organs were then harvested and frozen directly in Tissue-Tek OCT compound (VWR Scientific) using a dry ice/methylbutane bath, and stored at −70°C until cutting. Brains were fixed for a further 20 h at 4°C in 4% paraformaldehyde/PBS. Brains were then brought to 30% sucrose/0.1 M sodium phosphate, pH 7.4, at 4°C using steps of 10% sucrose for 1 h, 20% sucrose for 8 h, and finally 30% sucrose for 16 h. Finally, brains were frozen on dry ice and stored at −70°C until cutting.

Brain sections were cut at 30-μm thickness into PBS before staining for β-galactosidase in 24-well plates with HistoMark X-Gal solution (KPL) at 37°C for 16–20 h. The sections were then washed in PBS and mounted onto silanized slides with Clearmount (Zymed Laboratories). Other tissues were cut at 10-μm thickness onto silanized slides, fixed in cold acetone for 10 min, and then stored at −70°C until use. Slides were then stained as above after thawing and rehydration in PBS.

Humoral Challenge and Spleen Immunohistology. Chicken γ-globulin (CG; Sigma-Aldrich) was conjugated with (4-hydroxy-3-nitrophenyl; NP) acetyl succinimide ester (Calbiochem) in 0.1 M sodium borate, pH 9.2, to an NP/CG molar ratio of 13:1 ($NP_{13}CG$), and then dialyzed against PBS. Mice 6–8 wk of age were then challenged intraperitoneally with 50 μg of $NP_{13}CG$ adsorbed to alum in 0.1 ml PBS. Spleens were harvested at day 10 after the challenge, frozen in Tissue-Tek OCT compound using a dry ice/methylbutane bath, and stored at −70°C until cutting. Sections of 7-μm thickness were cut onto silanized glass slides, fixed in cold acetone for 10 min, air dried, and then stored at −70°C until use. For staining, sections were thawed for 30 min and then rehydrated in PBS for 20 min. Endogenous peroxidase was quenched with 0.3% hydrogen peroxide for 5 min. Sections were washed in PBS for 10 min and then preblocked with PBS/3% BSA/0.1% Tween 20 for 30 min in a humidified chamber. Staining for IgD was with rat anti-IgD (11–26) (Southern Biotechnology Associates, Inc.) and then horseradish peroxidase–conjugated polyclonal goat anti-rat IgG (Southern Biotechnology Associates, Inc.). Germinal centers were stained with biotin-conjugated peanut agglutinin (PNA) (EY Labs; reference 55). The presence of VCAM-1 was assessed with anti–VCAM-1 (M/K-2, rat IgG1, κ)-biotin (Southern Biotechnology Associates, Inc.). Anti-CD8b.2 (53-5.8, rat IgG1, κ)-biotin was used as a negative control for VCAM-1 staining. All biotin conjugates employed a secondary step of alkaline phosphatase–conjugated streptavidin (Zymed Laboratories). Incubations were in a humidified chamber for 1 h. Washes between steps were with PBS/0.1% Tween 20. Substrates for horseradish peroxidase and alkaline phosphatase were diaminobenzidine (Zymed Laboratories) and NBT/BCIP (Zymed Laboratories). Mounting was with Clearmount (Zymed Laboratories).

Spleen Collagenase Digestion. Spleens were harvested into 2 ml digest buffer in a 35-mm dish on ice. Digest buffer was calcium-free HBSS with 1% FCS, 2 mM L-glutamine, 0.5 mg/ml collagenase type IV (Sigma-Aldrich), and 0.1 mg/ml deoxyribonuclease type I (Sigma-Aldrich). Spleens were diced with 23-gauge needles before incubation at 37°C for 30 min. The cell suspension was further disrupted by pipetting before being made up to 10 ml with PBS/5 mM EDTA. Splenocytes were then centrifuged at 1,000 rpm for 5 min and resuspended into 2 ml ACK erythroid cell lysis buffer (BioWhittaker). 1 min later, the suspension was again made to 10 ml with PBS/5 mM EDTA and recentrifuged. Finally, cells were resuspended in PBS/1% FCS and filtered through 0.1-mm nylon mesh (Millipore).

Fluorocytometry. For fluorocytometry of DCs, cells were pre-

pared from spleen by collagenase digestion as described above. Otherwise, cells were recovered into 5 ml PBS/1% FCS from thymus, Peyer's patches, spleen, and/or LNs by using the plunger of a syringe to tease the tissue between two pieces of 0.1-mm nylon mesh (Millipore). Total BM was collected from femurs and tibias. Splenocytes were further treated by centrifugation at 1,000 rpm for 5 min, resuspension into 2 ml ACK erythroid cell lysis buffer (BioWhittaker), and then addition of 10 ml PBS 1 min later. All cell suspensions were then centrifuged at 1,000 rpm for 5 min. Finally, cells were resuspended into PBS/1% FCS and filtered through 0.1-mm nylon mesh. BM was not subjected to erythroid cell lysis, but total nucleated cell numbers in both BM and EDTA-treated blood were determined by counting in Turk's solution (0.01% wt/vol gentian violet in 3% vol/vol glacial acetic acid).

Aliquots of 10^6 nucleated cells were made into 0.2 ml PBS/1% FCS supplemented with 5 μg/ml FcBlock (BD PharMingen). Samples were left on ice for 30 min before primary antibodies were added and left on ice in the dark for another 1 h. Samples were washed by the addition of 1 ml PBS/1% FCS and centrifugation at 1,000 rpm, 4°C for 5 min. Secondary antibody incubation and washing were as above. Four-color fluorocytometry employed a FACSCalibur™ with argon and red diode lasers (Becton Dickinson). Fluorocytometry of spleen DCs, BM cells, and 5-chloromethylfluorescein diacetate (CMFDA)-labeled cells (see below) was done by counting 250,000 events. Otherwise, 50,000 events were collected.

Anti–mouse IgM (donkey polyclonal)-Cy5 and antidigoxin (mouse IgG polyclonal)-Cy5 were from Jackson ImmunoResearch Laboratories. Anti-IgD (11-26c.2a)-digoxigenin was made and employed by us as described previously (56). All other reagents were from BD PharMingen.

In Vivo Lymphocyte Homing Assay. C57BL/6J and *tcrα*$^{-/-}$ mice were purchased from The Jackson Laboratory and breeding colonies were maintained in our animal facility according to institutional animal care and use guidelines. Cells to be labeled were either LN (axillary, brachial, inguinal, and mesenteric) cells from C57BL/6J mice, splenocytes from *tcrα*$^{-/-}$ mice (after erythroid cell lysis and washing as described earlier), or preactivated T cells. The latter were prepared by culturing LN and spleen cells from C57BL/6J mice (after erythroid cell lysis and washing as described above) for 3 d at 5×10^6 cells/ml in DMEM supplemented with 2 mM glutamine, 50 μM 2-mercaptoethanol, 100 IU/ml penicillin, 0.1 mg/ml streptomycin, 5% FCS, 1 μg/ml anti-CD3 antibody (clone 2C11; Southern Biotechnology Associates, Inc.), and 50 U/ml IL-2. Cells were then washed and rested for a further 3 d in the same medium but without anti-CD3 antibody. Finally, dead cells were removed by centrifugation through lymphocyte separation medium (BioWhittaker).

Cells were labeled with 1 μM CMFDA succinimidyl ester (Molecular Probes) in PBS/0.1% BSA for 5 min at 37°C, and then washed three times with PBS by centrifugation at 1,000 rpm for 5–10 min. Finally, labeled cells were made to 2×10^8/ml in PBS and each 8–10-wk-old recipient was given 0.1 ml intravenously. 2 h later, peripheral blood, spleen, PLNs (axillary, brachial, and inguinal LNs), MLNs, and BM (femurs and tibias) were harvested for fluorocytometry as described above, with 250,000 events being counted per sample.

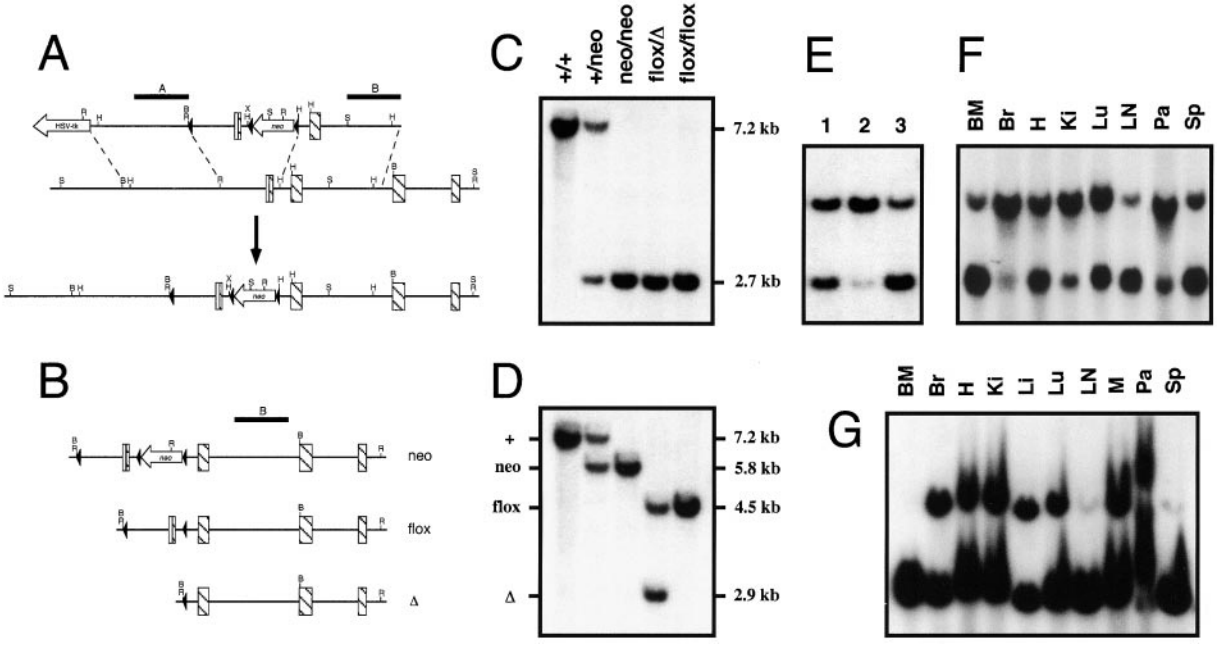

Figure 1. Targeting strategy and conditional deletion of the *vcam-1*^{flox} allele. (A) VCAM-1 knock-in mice (bottom locus map) contain Cre recombinase sites of recombination (*loxP* sites; black arrowheads). The *vcam-1* coding sequence exons are depicted as striped bars, with the 5′ untranslated region as a white bar. Probes A and B are shown above the top map line as black bars. Endonuclease sites shown are BamHI (B), EcoRI (R), HindIII (H), SphI (S), and XhoI (X). (B) The *vcam-1*^{neo} allele (neo) is shown along with two of the possible outcomes of Cre recombinase–mediated deletion, the *vcam-1*^{flox} allele (flox) and the *vcam-1*^{Δ} allele (Δ). (C and D) BamHI Southern blot analysis of tail DNA using probes A and B, respectively. Deletion of the *vcam-1*^{neo} allele to generate the *vcam-1*^{flox} allele (flox) and the *vcam-1*^{Δ} allele (Δ) in whole mice was achieved by interbreeding with the *splicer* transgene. (E) Southern blot analysis of mouse tail DNA as in D. A *vcam-1*$^{flox/Δ}$ mouse (track 1) is shown alongside two TIE2Cre$^+$ mice born of *vcam-1*$^{flox/flox}$ parents, but with the TIE2Cre$^+$ parent being the father (track 2) or mother (tracks 1 and 3). (F and G) Southern blot analysis as in D of genomic DNA from a *vcam-1*$^{flox/flox}$/TIE2Cre$^+$ mouse and a *vcam-1*$^{flox/Δ}$/TIE2Cre$^+$ mouse, respectively. Tissues analyzed were: BM; Br, brain (cortex); H, heart; Ki, kidney; Li, liver; Lu, lung; LNs; M, muscle (thigh); Pa, pancreas; and Sp, spleen.

Results

Generation of Conditional vcam-1–deficient Mice. Mice bearing Cre recombinase *loxP* sites of recombination were generated by homologous recombination in 129/Ola ES cells using conventional techniques (Fig. 1). The *vcam-1* region flanked by *loxP* sites includes the defined cytokine-responsive promoter region (49) and exon 1, with the *loxP*-flanked neomycin resistance cassette in intron 1. Exon 1 contains the signal peptide sequence and is critical to all the alternatively spliced forms of *vcam-1* (49–51). This region of *vcam-1* was previously deleted in mice using conventional techniques and resulted in embryonic lethality, as described by others (31, 48). Thus, the targeting strategy employed here was believed to be appropriate for achieving *vcam-1* inactivation, once the *loxP*-flanked region is deleted. The neomycin resistance cassette was removed by use of the *splicer* mouse (see Materials and Methods) to avoid any possible interference of VCAM-1 expression. Indeed, *vcam-1*$^{neo/neo}$ mice had four- to fivefold lower VCAM-1 on spleen DCs compared with *vcam-1*$^{flox/flox}$ mice and C57BL/6J mice (data not shown).

Conditional deletion of the *vcam-1*^{flox} allele (see Fig. 1 B for definitions) was achieved with a TIE2Cre Cre recombinase transgene. The latter was generated with the TIE2 kinase promoter/enhancer expression cassette, which gives uniform expression in all ECs during both embryogenesis and adulthood (53). When both parents had a *vcam-1*$^{flox/flox}$ genotype and the TIE2Cre^{+} parent was a female, all of the progeny had a *vcam-1*$^{flox/\Delta}$ genotype regardless of whether or not they themselves were TIE2Cre^{+} (Fig. 1 E). Thus, the TIE2Cre transgene appeared to delete the *vcam-1*^{flox} allele in the germline of the mother.

Both *vcam-1*$^{flox/flox}$/TIE2Cre^{+} mice (born with the TIE2Cre^{+} parent being the father) and *vcam-1*$^{flox/\Delta}$/TIE2Cre^{+} mice had extensive deletion of the *vcam-1*^{flox} allele in several tissues, but especially in tissues rich in hematopoietic cells (Fig. 1, F and G). This was anticipated because de novo TIE2 kinase is expressed by hematopoietic progenitors and ECs (57, 58). Virtually 100% deletion was seen in the BM of *vcam-1*$^{flox/\Delta}$/TIE2Cre^{+} mice (Fig. 1 G).

The high degree of deletion in lung tissue of *vcam-1*$^{flox/flox}$/TIE2Cre^{+} mice was reflected by a complete lack of VCAM-1 on lung ECs of *vcam-1*$^{flox/flox}$/TIE2Cre^{+} mice after OVA sensitization and aerosol challenge, which upregulates VCAM-1 expression in the lung (Fig. 2 A). VCAM-1 expression was also examined on BM myeloid lineage cells, spleen myeloid DCs, and spleen lymphoid DCs by fluorocytometry. This revealed relatively normal levels of VCAM-1 in *vcam-1*$^{flox/flox}$ mice (Fig. 2 B), whereas *vcam-1*$^{neo/neo}$ mice had four- to fivefold lower VCAM-1 (data not shown). VCAM-1 levels were greatly reduced in *vcam-1*$^{flox/flox}$/TIE2Cre^{+} mice, but complete deletion was achieved only in *vcam-1*$^{flox/\Delta}$/TIE2Cre^{+} mice (Fig. 2 B). As illustrated below (see Fig. 6), VCAM-1 was also deleted from spleen red pulp macrophages.

Finally, ROSA26R mice (54) were employed to further visualize deletion by the TIE2Cre transgene. ROSA26R mice express β-galactosidase only after Cre recombinase–mediated deletion of a "STOP" signal, and thus allow a histological evaluation of sites of Cre recombinase activity by staining for β-galactosidase activity (54). Thus, male TIE2Cre^{+} mice were crossed with ROSA26R mice (54) to obtain double-positive and ROSA26R^{+}/TIE2Cre^{-} progeny. Double-positive mice clearly revealed Cre recombinase activity as blue staining in the ECs of brain, kid-

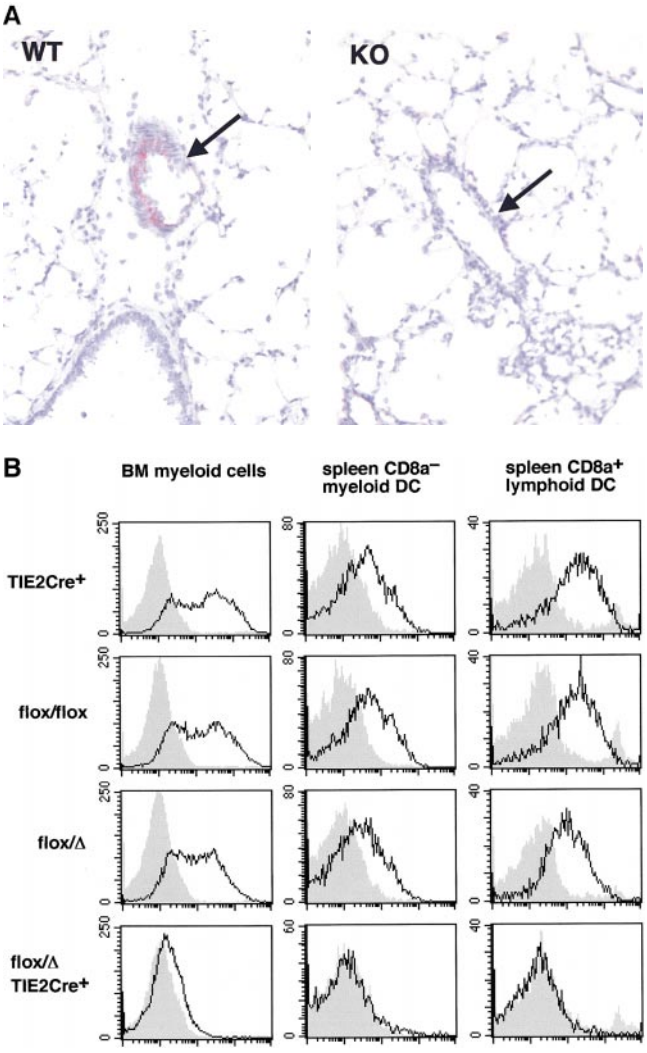

Figure 2. Cre recombinase–mediated deletion in ECs and hematopoietic cells. (A) Lung sections are shown for a *vcam-1*$^{+/+}$ mouse (WT) and a *vcam-1*$^{flox/flox}$/TIE2Cre^{+} mouse (KO) after OVA sensitization and aerosol challenge. A representative blood vessel is shown in each panel (arrow); original magnification: ×500. VCAM-1 staining is seen on ECs of the *vcam-1*$^{+/+}$ mouse lung (red) but not on ECs of the *vcam-1*$^{flox/flox}$/TIE2Cre^{+} mouse lung. (B) VCAM-1 (open histograms) was assessed on BM B220^{-} myeloid lineage cells (i.e., excluding high side-scatter granuloid cells and low forward-scatter erythroid cells, spleen CD11c^{+}CD8a^{-} myeloid DCs, and spleen CD11c^{+}CD8a^{+} lymphoid DCs by fluorocytometry. Anti-CD8b.2 (clone 53-5.8) was used as an isotype control (shaded histograms). The small peak of CD8b.2^{+} cells among CD11c^{+}CD8a^{+} splenocytes is expected, since it is known that a small fraction of CD8^{+} T cells are CD11c^{+}.

ney, LNs, spleen, and thymus (Fig. 3), while no staining was seen in ROSA26R$^+$/TIE2Cre$^-$ mice (data not shown). The blue staining of capillaries seen in the brain and thymus sections was typical. The intense blue staining of HEVs in the axillary LNs shown was typical of HEVs, and was also representative of thymic LNs and MLNs (data not shown). The relatively high staining intensity seen with HEV cells is presumably a reflection of the degree of β-galactosidase expression driven by the ROSA26R reporter promoter. It is not a reflection of more or less Cre recombinase–mediated deletion of the ROSA26R reporter allele because there is only one ROSA26R allele per cell. The completeness of deletion among HEV cells is witnessed at least by the blue coloration of the entire circumference of HEVs in every example seen. There was also consistent staining of arterioles and larger vessels in spleen sections and uniform staining of B cell follicles, in agreement with the earlier observation of complete deletion of the *vcam-1*^{flox} allele in hematopoietic cells. The apparent lack of staining in T cell areas of LNs and spleen as well as the thymus medulla may be due to the fact that T cells have a β-galactosidase inhibitory activity, as noted by others (59).

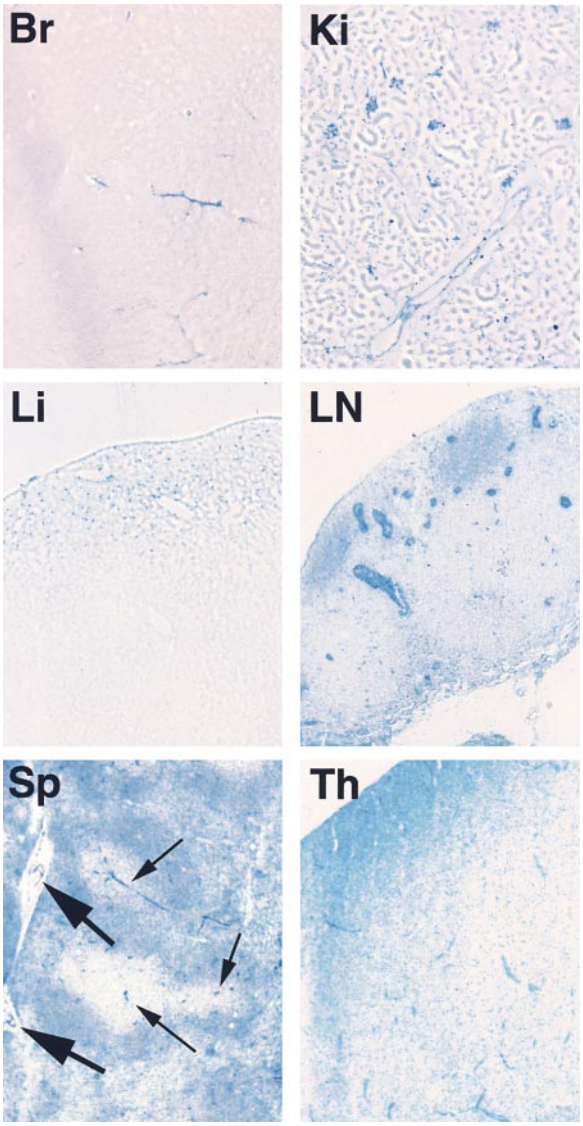

Figure 3. The TIE2Cre transgene activates the ROSA26R reporter allele and results in β-galactosidase activity in brain (Br), kidney (Ki), liver (Li), axillary LNs (LN), spleen (Sp), and thymus (Th), revealed by blue X-Gal staining (original magnification: ×100). Brain sections were 30 μm thick while all others were 10 μm. By way of example, thick and thin arrows in the spleen section indicate some larger vessels and arterioles, respectively.

Altered Lymphocyte Populations in Peripheral Blood and the BM Compartment. Fluorocytometry of cells from thymus, spleen, MLNs, PLNs (axillary, brachial, and inguinal), and Peyer's patches of *vcam-1*$^{flox/flox}$ and *vcam-1*$^{flox/\Delta}$/TIE2Cre$^+$ mice did not reveal any significant differences in leukocyte types or absolute numbers (data not shown). However, analysis of peripheral blood revealed mild leukocytosis in *vcam-1*$^{flox/\Delta}$/TIE2Cre$^+$ mice, including elevated levels of B220$^+$IgD^{lo}IgM^{hi} immature B cells (Fig. 4). Peripheral blood granuloid cells were also elevated in *vcam-1*$^{flox/\Delta}$/TIE2Cre$^+$ mice compared with their *vcam-1*$^{flox/\Delta}$/TIE2Cre$^-$ littermates, although this was not statistically significant compared with the age- and sex-matched *vcam-1*$^{flox/flox}$ mice.

Examination of BM from *vcam-1*$^{flox/\Delta}$/TIE2Cre$^+$ mice revealed a significant reduction in IgD^{lo}IgM^{hi} immature B cells (Fig. 5). However, there was no significant difference in numbers of B220$^+$CD43$^+$ pro-B cells (60), which represented ~5% of total nucleated BM cells in both *vcam-1*$^{flox/flox}$ mice and *vcam-1*$^{flox/\Delta}$/TIE2Cre$^+$ mice (Fig. 5). IgD$^+$ B cells and CD8$^+$ T cells were also reduced compared with *vcam-1*$^{flox/flox}$ mice, with a small but statistically insignificant reduction in total B220$^+$ B cells and CD4$^+$ T cells (Fig. 5). Total nucleated BM cell numbers were very similar in the

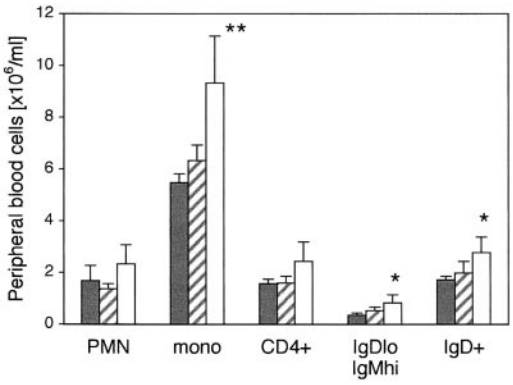

Figure 4. Peripheral blood analysis reveals leukocytosis in *vcam-1*$^{flox/\Delta}$/TIE2Cre$^+$ mice. A representative experiment (n = 5 per group) with age- and sex-matched *vcam-1*$^{flox/flox}$ mice (black bars), *vcam-1*$^{flox/\Delta}$/TIE2Cre$^-$ mice (striped bars), and their *vcam-1*$^{flox/\Delta}$/TIE2Cre$^+$ littermates (white bars). Total leukocyte numbers were determined from EDTA-treated blood in Turk's solution and are shown in millions of cells per milliliter of blood. Differential counts were established by fluorocytometry. PMNs were defined on the basis of high side-scatter, with the other cells defined as mononuclear (mono). The numbers of CD4$^+$ T cells, IgD^{lo}IgM^{hi} immature B cells, and IgD$^+$ B cells shown on the right are not in addition to the mononuclear cell counts but are part of the latter. Significant differences between *vcam-1*$^{flox/flox}$ mice and *vcam-1*$^{flox/\Delta}$/TIE2Cre$^+$ mice are indicated (Student's t test, *$P < 0.05$; **$P < 0.01$).

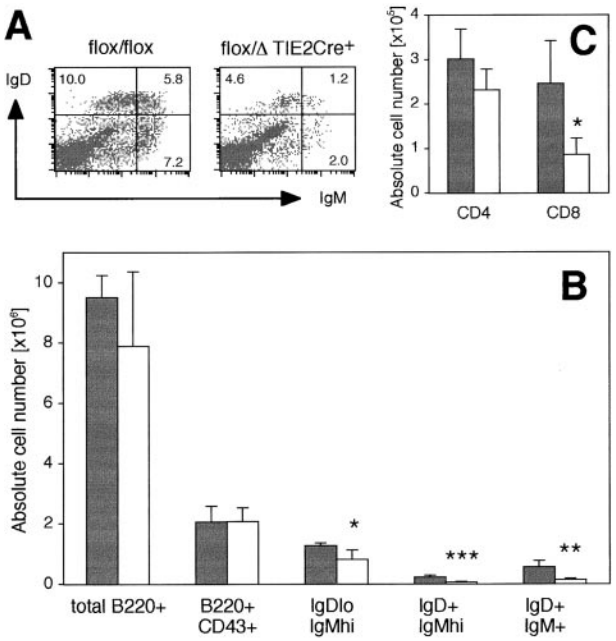

Figure 5. Reduced lymphocytes in BM of *vcam-1*$^{flox/\Delta}$/TIE2Cre^{+} mice. (A) Representative IgD versus IgM profile of B220^{+} cells in the BM of a *vcam-1*$^{flox/flox}$ mouse and a *vcam-1*$^{flox/\Delta}$/TIE2Cre^{+} mouse showing reduced IgD^{lo}IgM^{hi} immature B cells and IgD^{+} B cells in the latter. (B and C) Absolute lymphocyte numbers in the BM of age- and sex-matched *vcam-1*$^{flox/flox}$ mice (black bars) and *vcam-1*$^{flox/\Delta}$/TIE2Cre^{+} mice (white bars), showing normal B220^{+}CD43^{+} pro-B cell numbers but reduced numbers of other lymphocyte types. Significant differences between the two groups ($n = 4$ each) are indicated (Student's t test, $^{*}P < 0.02$; $^{**}P < 0.01$; $^{***}P < 0.002$).

above typical experiment, at 4.15 ± 0.52 × 10^7 cells and 4.14 ± 0.72 × 10^7 cells in *vcam-1*$^{flox/flox}$ mice and *vcam-1*$^{flox/\Delta}$/TIE2Cre^{+} mice ($n = 4$ mice per group), respectively. The combined reduction of lymphocyte numbers seen in *vcam-1*$^{flox/\Delta}$/TIE2Cre^{+} mice amounted to ~0.3 × 10^7 BM cells per mouse, and was therefore less than the standard deviation of the total nucleated BM cell numbers.

The apparently reduced levels of CD8^{+} T cells in BM were not obviously because of a selective loss of CD44^{hi}CD62L^{lo} memory cells, CD44^{hi}CD62L^{hi} "preactivated/experienced" cells, or CD44^{lo}CD62L^{hi} naive cells. In both *vcam-1*$^{flox/flox}$ mice and *vcam-1*$^{flox/\Delta}$/TIE2Cre^{+} mice, naive cells represented approximately one third of BM CD8^{+} T cells (data not shown). On the other hand, the small but statistically insignificant reduction in BM CD4^{+} T cells also revealed a significant reduction in the naive fraction of these cells. That is, naive CD4^{+} T cells represented 10.6 ± 4.0 and 5.2 ± 2.9% of total BM CD4^{+} T cells in *vcam-1*$^{flox/flox}$ mice and *vcam-1*$^{flox/\Delta}$/TIE2Cre^{+} mice, respectively (Student's t test, $P < 0.05$). This translated to absolute numbers of BM naive CD4^{+} T cells in the above typical experiment ($n = 4$ mice per group) of 3,282 ± 1,597 and 1,240 ± 729 cells in *vcam-1*$^{flox/flox}$ mice and *vcam-1*$^{flox/\Delta}$/TIE2Cre^{+} mice, respectively (Student's t test, $P < 0.05$).

Normal Humoral Responses in Conditional vcam-1–deficient Mice. Despite the reduced frequency of immature B cells in the BM of *vcam-1*$^{flox/\Delta}$/TIE2Cre^{+} mice and their increased numbers in peripheral blood, *vcam-1*$^{flox/\Delta}$/TIE2Cre^{+} mice showed relatively normal spleen B cell follicles with robust germinal center (GC) formation upon intraperitoneal challenge with NP_{13}CG adsorbed to alum (Fig. 6). There was also no significant difference in anti-NP IgG1 levels in the serum of *vcam-1*$^{flox/flox}$ mice ($n = 4$) versus *vcam-1*$^{flox/\Delta}$/TIE2Cre^{+} mice ($n = 8$) at days 10 and 35 after challenge (data not shown). Finally, the latter mice were given a booster injection of 0.2 mg soluble NP_{13}CG in PBS at day 35 after the challenge and serum anti-NP IgG1 was determined 6 d later. A significant difference was not seen between the two groups of mice (data not shown).

Of note is the fact that *vcam-1*$^{flox/\Delta}$/TIE2Cre^{+} mice still had VCAM-1 on follicular dendritic cells (FDCs) (Fig. 6). Also, VCAM-1 was not completely absent from the spleen red pulp compared with the negative staining by the anti-CD8b control (Fig. 6), presumably a result of VCAM-1 expression by spleen stromal cells (29, 30).

Impaired Lymphocyte Migration to BM. Having observed reduced lymphocyte numbers in BM, short-term migration assays were performed with CMFDA-labeled lymphocytes from LNs of C57BL/6J donor mice. The absolute numbers of CMFDA-labeled cells recovered from the spleens of *vcam-1*$^{flox/flox}$ recipients versus *vcam-1*$^{flox/\Delta}$/TIE2Cre^{+} recipients were not significantly different (data not shown). The fractions of CMFDA-labeled cells recovered in spleen, MLNs, and PLNs were also similar in the two groups of mice, but *vcam-1*$^{flox/\Delta}$/TIE2Cre^{+} mice clearly had greatly reduced CMFDA-labeled cells in BM (Fig. 7). Short-term migration of IgD^{+}, CD4^{+}, and CD8^{+} cells to the BM compartment of *vcam-1*$^{flox/\Delta}$/TIE2Cre^{+} recipients was reduced on average by ~93, 74, and 77% compared with the *vcam-1*$^{flox/flox}$ recipients, respectively. The actual frequencies of CMFDA-labeled IgD^{+} cells among total nucleated BM cells in *vcam-1*$^{flox/flox}$ recipients and *vcam-1*$^{flox/\Delta}$/TIE2Cre^{+} recipients were 0.118 ± 0.022 and 0.008 ± 0.002%, respectively.

Short-term migration assays were also performed with CMFDA-labeled splenocytes from *tcrα*$^{-/-}$ donors, revealing that the reduced short-term migration to BM by IgD^{+} B cells was also true of other B cell subsets (Fig. 8). This reduced short-term migration to BM was reflected in elevated cell numbers in peripheral blood (Fig. 8). The exact identity of the cells among the IgD^{lo}IgM^{hi} subset that had either homed to BM or remained in peripheral blood was not determined, but these cells might have included marginal zone memory B cells and/or immature "transitional" B cells.

To further dissect the requirement for VCAM-1 in CD4^{+} T cell migration, short-term migration assays were then performed with preactivated/experienced T cells (Fig. 9). This revealed greatly impaired short-term migration to BM of *vcam-1*$^{flox/\Delta}$/TIE2Cre^{+} mice by both CD4^{+}CD62L^{hi} T cells and CD4^{+}CD62L^{lo} T cells (75 and 70% reduction, respectively). The absolute numbers of CMFDA-labeled cells in spleen and PLNs mirrored the earlier results, with no apparent difference (Fig. 9). Also, as might be expected, CD4^{+}CD62L^{hi} cells preferentially homed to PLNs compared with CD4^{+}CD62L^{lo} cells (Fig. 9).

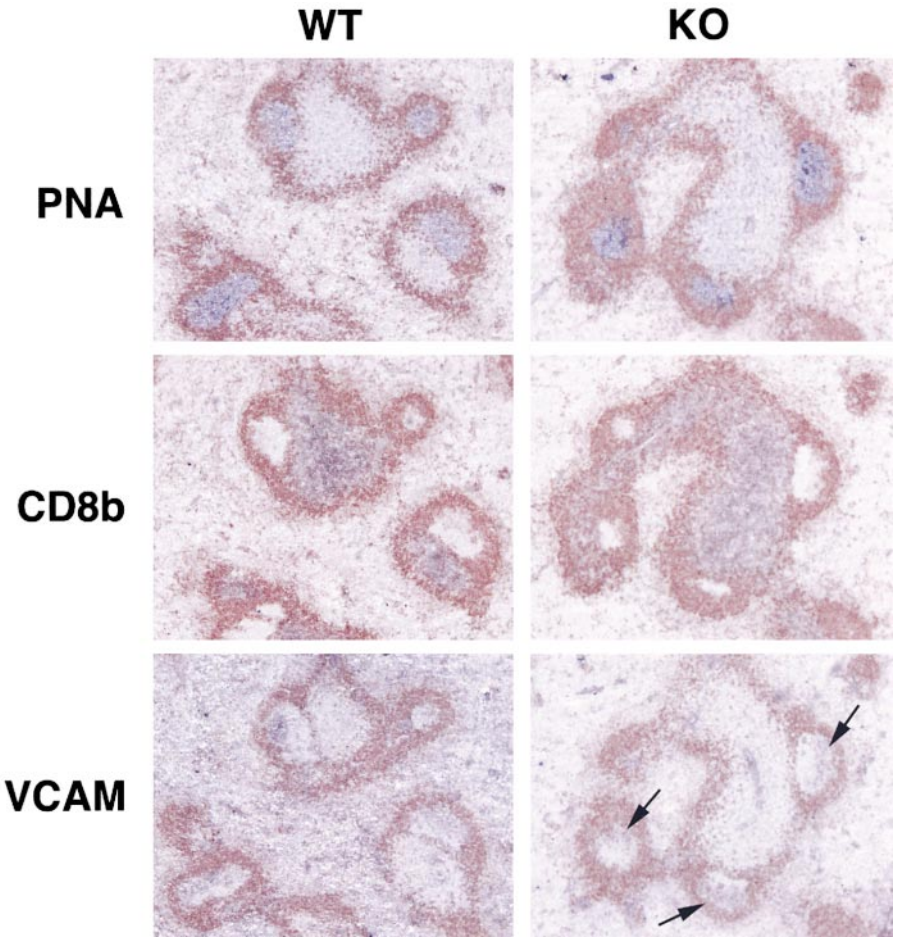

Figure 6. Relatively normal B cell responses in *vcam-1*$^{flox/\Delta}$/TIE2Cre^{+} mice. Serial spleen sections from a *vcam-1*$^{flox/flox}$ mouse (WT) and a *vcam-1*$^{flox/\Delta}$/TIE2Cre^{+} mouse (KO) 10 d after intraperitoneal challenge with $NP_{13}CG$ adsorbed to alum (original magnifications: ×100). All sections were stained with anti-IgD antibody (seen in brown) and either PNA, anti-CD8b, or anti–VCAM-1. PNA, CD8b, and VCAM-1 staining are in purple. Arrows in the KO section indicate typical VCAM-1 staining on FDCs within GCs.

Discussion

We have employed the Cre recombinase/*loxP* system to generate *vcam-1* knock-in (*vcam-1*$^{flox/flox}$) mice. We also generated a Cre recombinase transgene (TIE2Cre) to delete this conditional *vcam-1* allele in whole mice. Analysis of sites of TIE2Cre activity with the ROSA26R reporter strain (54) showed the TIE2Cre transgene to be capable of mediating deletion in ECs of at least brain, kidney, LNs, spleen, and thymus. The β-galactosidase staining of HEV in LNs, for example, revealed TIE2Cre-mediated deletion in every single HEV cell (Fig. 3), suggesting 100% penetration by the transgene. Furthermore, virtually complete loss of VCAM-1 was seen on lung ECs, BM myeloid cells, spleen myeloid DCs, and spleen lymphoid DCs of *vcam-1*$^{flox/\Delta}$/TIE2Cre^{+} mice. The apparent absence of VCAM-1 cannot be explained as being a result of loss of only the anti–VCAM-1 antibody epitope (rather than VCAM-1 per se), because the deletion strategy employed does not remove any of the exons encoding the mature VCAM-1

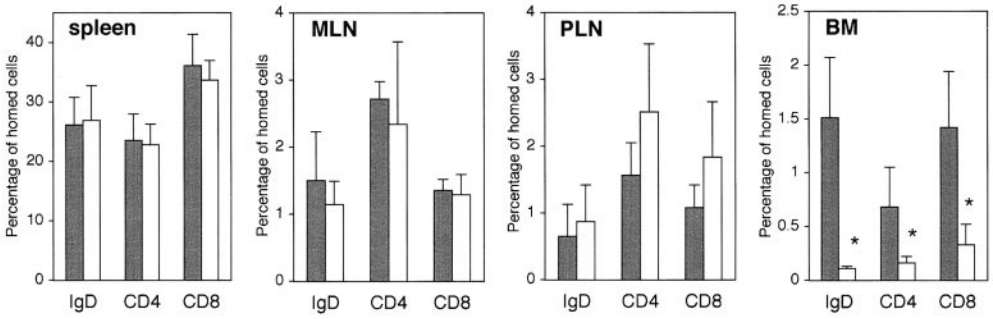

Figure 7. Reduced short-term lymphocyte migration to BM in *vcam-1*$^{flox/\Delta}$/TIE2Cre^{+} mice. A representative experiment with age- and sex-matched *vcam-1*$^{flox/flox}$ recipients (black bars) and *vcam-1*$^{flox/\Delta}$/TIE2Cre^{+} recipients (white bars). The frequency of CMFDA-labeled cells (IgD^{+}, CD4^{+}, and CD8a^{+}) was used to determine the absolute numbers of each type of CMFDA-labeled cell in each lymphoid organ. These data were then represented as the percentage of homed cells, where 100% is the total number of recovered CMFDA-labeled cells in each individual mouse ($n = 3$ per group). *Significantly different from controls (Student's *t* test, $P < 0.02$). The slightly elevated migration to PLNs of *vcam-1*$^{flox/\Delta}$/TIE2Cre^{+} recipients was not statistically significant.

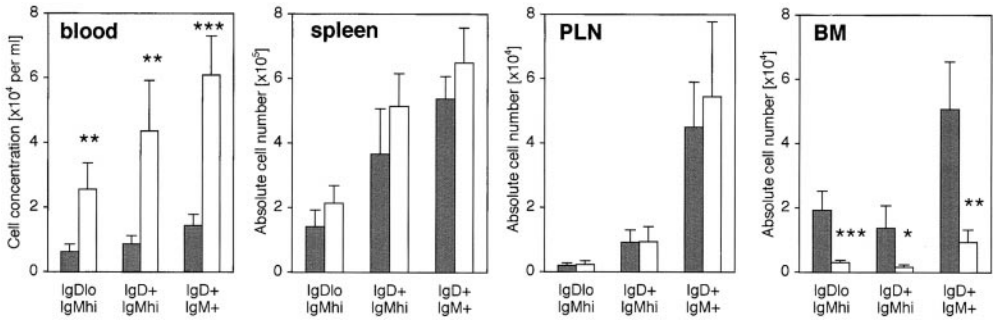

Figure 8. Impaired B cell recirculation to BM results in elevated peripheral blood levels. Age- and sex-matched *vcam-1*$^{flox/flox}$ recipients (black bars) and *vcam-1*$^{flox/\Delta}$/TIE2Cre^{+} recipients (white bars) received CMFDA-labeled splenocytes from *tcr*$\alpha^{-/-}$ donors, and recipient lymphoid organs and blood were harvested 2 h later ($n = 4$ per group). The IgD versus IgM profile of CMFDA-labeled cells was determined as in the legend to Fig. 5 A, and the frequency of CMFDA-labeled cells was used to determine the absolute numbers of each type of CMFDA-labeled cell in each lymphoid organ. Significant differences are indicated (Student's *t* test, $*P < 0.01$; $**P < 0.005$; $***P < 0.001$).

polypeptide. Rather, we have deleted the VCAM-1 promoter region and exon 1. The latter contains the signal peptide sequence and is critical to all of the alternatively spliced forms of *vcam-1* (49–51).

Our studies reveal a dominant role for VCAM-1 in lymphocyte migration to BM. Having said this, we have not yet definitively demonstrated that VCAM-1 is actually absent from BM ECs in *vcam-1*$^{flox/\Delta}$/TIE2Cre^{+} mice. Although we observed virtually 100% deletion of the *vcam-1*^{flox} allele in BM (Fig. 1 G), the vast majority of the BM genomic content is undoubtedly derived from hematopoietic cells. This issue will be addressed by the generation of BM EC lines as well as BM stromal cell lines. Nonetheless, short-term migration of B cells, CD4^{+} T cells, and CD8^{+} T cells to the BM of *vcam-1*$^{flox/\Delta}$/TIE2Cre^{+} mice was reduced on average by ~80, 74, and 77%, respectively. Also, short-term migration by CD4^{+}CD62L^{hi} and CD4^{+} CD62L^{lo} preactivated/experienced T cells was reduced on average by ~75 and 70%, respectively.

It is conceivable that the low levels of lymphocytes still found in the BM of *vcam-1*$^{flox/\Delta}$/TIE2Cre^{+} mice are a result of alternate or complimentary mechanisms of migration. Certainly, this would not be unprecedented. For example, ICAM-1–deficient mice show reduced but substantial contact hypersensitivity and neutrophil migration (61, 62). Likewise, LFA-1–deficient lymphocytes show reduced but not absent lymphocyte migration to PLNs, MLNs, and Peyer's patches (24, 63). Also, P/E-selectin double deficiency reduces hematopoietic progenitor cell rolling at BM microvessels to 30–40% of control levels (7). This selectin-independent rolling is further reduced ~70% by anti–VCAM-1 antibody, while anti–VCAM-1 antibody treatment of wild-type BM microvessels reduces hematopoietic progenitor cell rolling by only ~30% (7). Finally, anti–VCAM-1–antibody greatly reduces the migration of LFA-1–deficient lymphocytes to BM (24). We have shown that greatly reduced migration can also be achieved with VCAM-1 deficiency alone, and that this applies to all three major lymphocyte subsets. Taken together, these observations suggest that both LFA-1 receptors and VCAM-1 are involved in lymphocyte migration to BM, but that VCAM-1 plays a dominant role.

We have not yet definitively determined whether or not VCAM-1 is deleted from BM stromal cells of *vcam-1*$^{flox/\Delta}$/TIE2Cre^{+} mice. This is currently the subject of further investigation by the generation of BM stromal cell lines. This is of potential interest because VCAM-1 on BM stromal cells might prove to have a role in B cell development and/or humoral response beyond those that have been revealed by our *vcam-1*$^{flox/\Delta}$/TIE2Cre^{+} mice. For example, α_4 integrin–deficient hematopoietic progenitor cell chimeric mice had greatly reduced levels of α_4 integrin–deficient pre-B cells (36), and it has not yet been determined whether the α_4 integrin receptor involved in pre-B cell development is VCAM-1, fibronectin, or both. Also, anti–VCAM-1 antibody greatly reduced B lymphocyte formation in long-term bone marrow cultures (25). However, this is in contrast to studies with BM stromal cell clones from VCAM-1

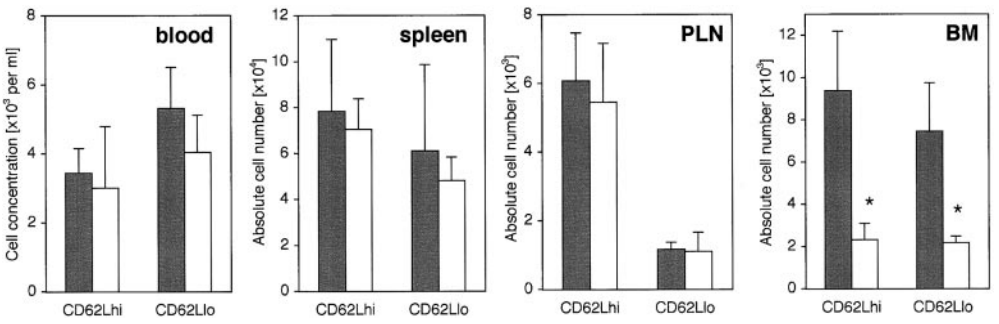

Figure 9. Reduced short-term migration by preactivated CD4^{+} T cells. Age- and sex-matched *vcam-1*$^{flox/flox}$ recipients (black bars) and *vcam-1*$^{flox/\Delta}$/TIE2Cre^{+} recipients (white bars) received CMFDA-labeled preactivated/experienced T cells as described in Materials and Methods, and recipient lymphoid organs and blood were harvested 2 h later ($n = 4$ per group). The CD4 versus CD62L profile of CMFDA-labeled cells was determined by fluorocytometry, and the frequency of CMFDA-labeled cells was used to determine the absolute numbers of each type of CMFDA-labeled cell in each lymphoid organ (note the differences in scale). Significant differences are indicated (Student's *t* test, $*P < 0.002$).

null mice where long-term maintenance and proliferation of clonable pre-B cells, cobblestone formation, and differentiation to IgM-secreting mature B cells were equally possible on VCAM-1^+ and VCAM-1^- stromal cells (35).

In this issue, Leuker et al. (64) have also generated conditional *vcam-1*–deficient mice using an IFN-inducible Cre recombinase system. These authors show that their *vcam-1*–deficient mice have a phenotype similar to our mice. In addition, they show relatively low antigen-specific serum antibody several weeks after challenge, after secondary challenge (64). We did not find reduced humoral responses in our mice (data not shown), perhaps due to differences in humoral challenge. Having said this, we anticipate that this difference in humoral response will be determined to be because of the nature of our respective conditional VCAM-1 deletion strategies. That is, the IFN-induced *vcam-1*–deficient mice of Leuker et al. might lack VCAM-1 on cells that our mice do not (e.g., FDCs, spleen stromal cells, and/or BM stromal cells). First, in vitro studies suggest that VCAM-1 on FDCs participates in adherence with, and prevents apoptosis of, GC B cells (65). Second, human spleen-derived stromal cells promote B cell blast differentiation and survival resulting in enhanced antibody secretion, in a manner that can be partly blocked by anti–VCAM-1 antibody (66). Third, BM fibroblasts can rescue cells from apoptosis (67), conceivably in a VCAM-1–dependent manner. As mentioned below, plasma cells are known to express the VCAM-1 ligand, VLA-4. Thus, antibody-secreting cell differentiation and/or longevity might be perturbed in mice lacking VCAM-1 on spleen and/or BM stromal cells.

Humoral responses in our mice are being further investigated, but clearly any difference between our mice and those of Leuker et al. (64) is not because of a lack of deletion of VCAM-1 on conventional DCs in our mice (Fig. 2 B).

In conclusion, we have generated conditional *vcam-1*–deficient mice and found them to have a reduced capacity to recruit lymphocytes to BM. Our short-term lymphocyte homing studies showed that migration to wild-type mouse BM (femur and tibia) represents ~3–5% of the total homed cells among the organs examined. Given that this represents only BM from femur and tibia, the total migration to BM probably represents a substantial fraction comparable in size to that seen in MLNs and PLNs. As suggested by others (24), perhaps BM should be considered as a major part of the lymphocyte recirculation network. Besides being a home for antibody secreting cells, the physiological relevance of lymphocyte recirculation to BM is not fully understood. The BM compartment is capable of functioning as a site of primary immune function under conditions of disrupted lymphocyte trafficking to spleen and LNs (68). It remains to be seen whether or not the BM compartment can act as a priming site in other physiological conditions. The pathophysiology of lymphocytes in BM, however, is perhaps better appreciated. BM is a major site of involvement in B and T cell malignancy (69), and metastasis to BM by lymphomas is often a very poor prognostic indicator. Both normal human plasma cells and myelomas express VLA-4 (70), and myelomas home to the BM where they induce massive osteoclastic bone destruction (71, 72). Anti–VCAM-1 antibody also greatly suppresses myeloma cell adhesion to BM ECs in vitro (73). Furthermore, direct cell–cell contact between myeloma cells and BM stromal cells via VCAM-1/VLA-4 is critical in some models to the production of destructive bone resorption (74). Finally, the most common symptoms in childhood acute leukemia, for example, are fever, infection, and bleeding resulting from neutropenia, anemia, and thrombocytopenia, which are secondary consequences of BM infiltration by leukemic cells (69). Thus, it might be beneficial to be able to prevent such cells from homing to and/or flourishing in the BM compartment.

We thank Christoph Leuker et al. for discussing with us their IFN-inducible conditional VCAM-1 knockout mice before publication. We are also indebted to Thomas Sato for the TIE2 kinase promoter/enhancer cassette. We also thank Linda Evangelisti, Debbie Butkus, and Cindy Hughes for their technical assistance and Fran Manzo and Ginny Chenell for secretarial assistance.

This work was supported by the Howard Hughes Medical Institute (to R. Flavell), a Human Frontier Science Program Long-Term Fellowship (to P. Koni), and a Mentor-Based American Diabetes Association Fellowship (to P. Koni). R. Flavell is an Investigator of the Howard Hughes Medical Institute.

Submitted: 19 July 2000
Revised: 5 January 2001
Accepted: 12 January 2001

References

1. Butcher, E.C. 1991. Leukocyte-endothelial cell recognition: three (or more) steps to specificity and diversity. *Cell.* 67: 1033–1036.
2. Bevilacqua, M.P. 1993. Endothelial-leukocyte adhesion molecules. *Annu. Rev. Immunol.* 11:767–804.
3. Springer, T.A. 1994. Traffic signals for lymphocyte recirculation and leukocyte emigration: the multistep paradigm. *Cell.* 2:301–314.
4. Berlin, C., R.F. Bargatze, J.J. Campbell, U.H. von Andrian, M.C. Szabo, S.R. Hasslen, R.D. Nelson, E.L. Berg, S.L. Erlandsen, and E.C. Butcher. 1995. α4 integrins mediate lymphocyte attachment and rolling under physiologic flow. *Cell.* 3:413–422.
5. Jones, D.A., L.V. McIntire, C.W. Smith, and L.J. Picker. 1994. A two-step adhesion cascade for T cell/endothelial cell interactions under flow conditions. *J. Clin. Invest.* 6:2443–2450.
6. Alon, R., P.D. Kassner, M.W. Carr, E.B. Finger, M.E. Hemler, and T.A. Springer. 1995. The integrin VLA-4 supports tethering and rolling in flow on VCAM-1. *J. Cell Biol.* 6:1243–1253.
7. Mazo, I.B., J.C. Gutierrez-Ramos, P.S. Frenette, R.O. Hynes, D.D. Wagner, and U.H. von Andrian. 1998. Hematopoietic progenitor cell rolling in bone marrow microvessels: parallel contributions by endothelial selectins and vascular cell adhesion molecule 1 [published erratum at 5: 1001]. *J. Exp. Med.* 3:465–474.
8. Osborn, L., C. Hession, R. Tizzard, C. Vassalio, S. Luhowskyj, G. Chi-Rosso, and R. Lobb. 1989. Direct expres-

sion cloning of vascular cell adhesion molecule 1, a cytokine-induced endothelial protein that binds to lymphocytes. *Cell.* 59:1203–1211.
9. Rice, G.E., and M.P. Bevilacqua. 1989. An inducible endothelial cell surface glycoprotein mediates melanoma adhesion. *Science.* 246:1303–1306.
10. Rice, G.E., J.M. Munro, and M.P. Bevilacqua. 1990. Inducible cell adhesion molecule 110 (INCAM-110) is an endothelial receptor for lymphocytes. A CD11/CD18-independent adhesion mechanism. *J. Exp. Med.* 4:1369–1374.
11. Neish, A.S., A.J. Williams, H.J. Palmer, M.Z. Whitley, and T. Collins. 1992. Functional analysis of the human vascular cell adhesion molecule 1 promoter. *J. Exp. Med.* 6:1583–1593.
12. Swerlick, R.A., K.H. Lee, L.J. Li, N.T. Sepp, S.W. Caughman, and T.J. Lawley. 1992. Regulation of vascular cell adhesion molecule 1 on human dermal microvascular endothelial cells. *J. Immunol.* 2:698–705.
13. Sironi, M., F.L. Sciacca, C. Matteucci, M. Conni, A. Vecchi, S. Bernasconi, A. Minty, D. Caput, P. Ferrara, F. Colotta, et al. 1994. Regulation of endothelial and mesothelial cell function by interleukin-13: selective induction of vascular cell adhesion molecule-1 and amplification of interleukin-6 production. *Blood.* 6:1913–1921.
14. Lawson, C., M. Ainsworth, M. Yacoub, and M. Rose. 1999. Ligation of ICAM-1 on endothelial cells leads to expression of VCAM-1 via a nuclear factor-κB-independent mechanism. *J. Immunol.* 5:2990–2996.
15. Briscoe, D.M., F.J. Schoen, G.E. Rice, M.P. Bevilacqua, P. Ganz, and J.S. Pober. 1991. Induced expression of endothelial-leukocyte adhesion molecules in human cardiac allografts. *Transplantation.* 51:537–539.
16. Cybulsky, M.I., and M.A. Gimbrone, Jr. 1991. Endothelial expression of a mononuclear leukocyte adhesion molecule during atherogenesis. *Science.* 251:788–791.
17. van Dinther-Janssen, A.M., E. Horst, G. Koopman, W. Newman, R.J. Scheper, C.M. Meijer, and S.T. Pals. 1991. The VLA-4/VCAM-1 pathway is involved in lymphocyte adhesion to endothelium in rheumatoid synovium. *J. Immunol.* 147:4207–4210.
18. Rice, G.E., J.M. Munro, C. Corless, and M.P. Bevilacqua. 1991. Vascular and nonvascular expression of INCAM-110. A target for mononuclear leukocyte adhesion in normal and inflamed human tissues. *Am. J. Pathol.* 2:385–393.
19. Koizumi, M., N. King, R. Lobb, C. Benjamin, and D.K. Podolsky. 1992. Expression of vascular adhesion molecules in inflammatory bowel disease. *Gastroenterology.* 3:840–847.
20. Brockmeyer, C., M. Ulbrecht, D.J. Schendel, E.H. Weiss, G. Hillerbrand, K. Burkhardt, W. Land, M.J. Gokel, G. Riethmuller, and H.E. Feucht. 1993. Distribution of cell adhesion molecules (ICAM-1, VCAM-1, ELAM-1) in renal tissue during allograft rejection. *Transplantation.* 55:610–615.
21. Ferran, C., M. Peuchmaur, M. Desruennes, J.J. Ghoussoub, A. Cabrol, N. Brousse, C. Cabrol, J.F. Bach, and L. Chatenoud. 1993. Implications of de novo ELAM-1 and VCAM-1 expression in human cardiac allograft rejection. *Transplantation.* 3:605–609.
22. O'Brien, K.D., M.D. Allen, T.O. McDonald, A. Chait, J.M. Harlan, D. Fishbein, J. McCarty, M. Ferguson, K. Hudkins, C.D. Benjamin, et al. 1993. Vascular cell adhesion molecule-1 is expressed in human coronary atherosclerotic plaques. Implications for the mode of progression of advanced coronary atherosclerosis. *J. Clin. Invest.* 92:945–951.
23. Raine, C.S. 1994. The Dale E. McFarlin Memorial Lecture: the immunology of the multiple sclerosis lesion. *Ann. Neurol.* 36(Suppl.):S61–S72.
24. Berlin-Rufenach, C., F. Otto, M. Mathies, J. Westermann, M.J. Owen, A. Hamann, and N. Hogg. 1999. Lymphocyte migration in lymphocyte function–associated antigen (LFA)-1–deficient mice. *J. Exp. Med.* 189:1467–1478.
25. Miyake, K., K. Medina, K. Ishihara, M. Kimoto, R. Auerbach, and P.W. Kincade. 1991. A VCAM-like adhesion molecule on murine bone marrow stromal cells mediates binding of lymphocyte precursors in culture. *J. Cell Biol.* 114:557–565.
26. Jacobsen, K., J. Kravitz, P.W. Kincade, and D.G. Osmond. 1996. Adhesion receptors on bone marrow stromal cells: in vivo expression of vascular cell adhesion molecule-1 by reticular cells and sinusoidal endothelium in normal and γ-irradiated mice. *Blood.* 1:73–82.
27. Schweitzer, K.M., A.M. Drager, P. van der Valk, S.F. Thijsen, A. Zevenbergen, A.P. Theijsmeijer, C.E. van der Schoot, and M.M. Langenhuijsen. 1996. Constitutive expression of E-selectin and vascular cell adhesion molecule-1 on endothelial cells of hematopoietic tissues. *Am. J. Pathol.* 1:165–175.
28. Salomon, D.R., L. Crisa, C.F. Mojcik, J.K. Ishii, G. Klier, and E.M. Shevach. 1997. Vascular cell adhesion molecule-1 is expressed by cortical thymic epithelial cells and mediates thymocyte adhesion. Implications for the function of α4β1 (VLA4) integrin in T-cell development. *Blood.* 89:2461–2471.
29. Borrello, M.A., and R.P. Phipps. 1996. Differential Thy-1 expression by splenic fibroblasts defines functionally distinct subsets. *Cell. Immunol.* 173:198–206.
30. Castro, A., M.R. Bono, V. Simon, L. Vargas, and M. Rosemblatt. 1997. Spleen-derived stromal cells. Adhesion molecules expression and lymphocyte adhesion to reticular cells. *Eur. J. Cell Biol.* 74:321–328.
31. Gurtner, G.C., V. Davis, H. Li, M.J. McCoy, A. Sharpe, and M.I. Cybulsky. 1995. Targeted disruption of the murine VCAM1 gene: essential role of VCAM-1 in chorioallantoic fusion and placentation. *Genes Dev.* 1:1–14.
32. Pulendran, B., J. Lingappa, M.K. Kennedy, J. Smith, M. Teepe, A. Rudensky, C.R. Maliszewski, and E. Maraskovsky. 1997. Developmental pathways of dendritic cells in vivo: distinct function, phenotype, and localization of dendritic cell subsets in FLT3 ligand-treated mice. *J. Immunol.* 5:2222–2231.
33. Ishiyama, N., M. Kitagawa, H. Takahashi, T. Kina, and K. Hirokawa. 1998. Expression of VCAM-1 in lymphocytes during the process of apoptosis. *Pathobiology.* 6:274–283.
34. Frenette, P.S., S. Subbarao, I.B. Mazo, U.H. von Andrian, and D.D. Wagner. 1998. Endothelial selectins and vascular cell adhesion molecule-1 promote hematopoietic progenitor homing to bone marrow. *Proc. Natl. Acad. Sci. USA.* 24: 14423–14428.
35. Friedrich, C., M.I. Cybulsky, and J.C. Gutierrez-Ramos. 1996. Vascular cell adhesion molecule-1 expression by hematopoiesis-supporting stromal cells is not essential for lymphoid or myeloid differentiation in vivo or in vitro. *Eur. J. Immunol.* 11:2773–2780.
36. Arroyo, A.G., J.T. Yang, H. Rayburn, and R.O. Hynes. 1999. α4 integrins regulate the proliferation/differentiation balance of multilineage hematopoietic progenitors in vivo. *Immunity.* 5:555–566.

37. Wayner, E.A., A. Garcia-Pardo, M.J. Humphries, J.A. McDonald, and W.G. Carter. 1989. Identification and characterization of the T lymphocyte adhesion receptor for an alternative cell attachment domain (CS-1) in plasma fibronectin. *J. Cell Biol.* 3:1321–3130.
38. Elices, M.J., L. Osborn, Y. Takada, C. Crouse, S. Luhowskyj, M.E. Hemler, and R.R. Lobb. 1990. VCAM-1 on activated endothelium interacts with the leukocyte integrin VLA-4 at a site distinct from the VLA-4/fibronectin binding site. *Cell.* 4:577–584.
39. Mould, A.P., L.A. Wheldon, A. Komoriya, E.A. Wayner, K.M. Yamada, and M.J. Humphries. 1990. Affinity chromatographic isolation of the melanoma adhesion receptor for the IIICS region of fibronectin and its identification as the integrin α4β1. *J. Biol. Chem.* 7:4020–4024.
40. Pulido, R., M.J. Elices, M.R. Campanero, L. Osborn, S. Schiffer, A. Garcia-Pardo, R. Lobb, M.E. Hemler, and F. Sanchez-Madrid. 1991. Functional evidence for three distinct and independently inhibitable adhesion activities mediated by the human integrin VLA-4. Correlation with distinct α4 epitopes. *J. Biol. Chem.* 16:10241–10245.
41. Chan, B.M., M.J. Elices, E. Murphy, and M.E. Hemler. 1992. Adhesion to vascular cell adhesion molecule 1 and fibronectin. Comparison of α4β1 (VLA-4) and α4β7 on the human B cell line JY. *J. Biol. Chem.* 12:8366–8370.
42. Ruegg, C., A.A. Postigo, E.E. Sikorski, E.C. Butcher, R. Pytela, and D.J. Erle. 1992. Role of integrin α4β7/α4β P in lymphocyte adherence to fibronectin and VCAM-1 and in homotypic cell clustering. *J. Cell Biol.* 1:179–189.
43. Irie, A., T. Kamata, W. Puzon-McLaughlin, and Y. Takada. 1995. Critical amino acid residues for ligand binding are clustered in a predicted β-turn of the third N-terminal repeat in the integrin α4 and α5 subunits. *EMBO (Eur. Mol. Biol. Organ.) J.* 22:5550–5556.
44. Altevogt, P., M. Hubbe, M. Ruppert, J. Lohr, P. von Hoegen, M. Sammar, D.P. Andrew, L. McEvoy, M.J. Humphries, and E.C. Butcher. 1995. The α4 integrin chain is a ligand for α4β7 and α4β1. *J. Exp. Med.* 2:345–355.
45. Grayson, M.H., M. Van der Vieren, S.A. Sterbinsky, W.M. Gallatin, P.A. Hoffman, D.E. Staunton, and B.S. Bochner. 1998. $\alpha_D\beta_2$ is expressed on human eosinophils and functions as an alternative ligand for vascular cell adhesion molecule 1 (VCAM-1). *J. Exp. Med.* 188:2187–2191.
46. Van der Vieren, M., D.T. Crowe, D. Hoekstra, R. Vazeux, P.A. Hoffman, M.H. Grayson, B.S. Bochner, W.M. Gallatin, and D.E. Staunton. 1999. The leukocyte integrin $\alpha_D\beta_2$ binds VCAM-1: evidence for a binding interface between I domain and VCAM-1. *J. Immunol.* 163:1984–1990.
47. Taooka, Y., J. Chen, T. Yednock, and D. Sheppard. 1999. The integrin α9β1 mediates adhesion to activated endothelial cells and transendothelial neutrophil migration through interaction with vascular cell adhesion molecule-1. *J. Cell Biol.* 145:413–420.
48. Kwee, L., H.S. Baldwin, H.M. Shen, C.L. Stewart, C. Buck, C.A. Buck, and M.A. Labow. 1995. Defective development of the embryonic and extraembryonic circulatory systems in vascular cell adhesion molecule (VCAM-1) deficient mice. *Development.* 2:489–503.
49. Cybulsky, M.I., M. Allan-Motamed, and T. Collins. 1993. Structure of the murine VCAM1 gene. *Genomics.* 2:387–391.
50. Terry, R.W., L. Kwee, J.F. Levine, and M.A. Labow. 1993. Cytokine induction of an alternatively spliced murine vascular cell adhesion molecule (VCAM) mRNA encoding a glycosylphosphatidylinositol-anchored VCAM protein. *Proc. Natl. Acad. Sci. USA.* 13:5919–5923.
51. Kumar, A.G., X.Y. Dai, C.A. Kozak, M.P. Mims, A.M. Gotto, and C.M. Ballantyne. 1994. Murine VCAM-1. Molecular cloning, mapping, and analysis of a truncated form. *J. Immunol.* 9:4088–4098.
52. McKnight, S.L. 1980. The nucleotide sequence and transcript map of the herpes simplex virus thymidine kinase gene. *Nucleic Acids Res.* 8:5949–5964.
53. Schlaeger, T.M., S. Bartunkova, J.A. Lawitts, G. Teichmann, W. Risau, U. Deutsch, and T.N. Sato. 1997. Uniform vascular-endothelial-cell-specific gene expression in both embryonic and adult transgenic mice. *Proc. Natl. Acad. Sci. USA.* 7:3058–3063.
54. Soriano, P. 1999. Generalized lacZ expression with the ROSA26 Cre reporter strain. *Nat. Genet.* 21:70–71.
55. Rose, M.L., M.S.C. Birbeck, V.J. Wallis, J.A. Forrester, and A.J.S. Davies. 1980. Peanut lectin binding properties of germinal centres of mouse lymphoid tissue. *Nature.* 284:364–366.
56. Koni, P.A., and R.A. Flavell. 1999. Lymph node germinal centers form in the absence of follicular dendritic cell networks. *J. Exp. Med.* 189:855–864.
57. Batard, P., P. Sansilvestri, C. Scheinecker, W. Knapp, N. Debili, W. Vainchenker, H.J. Buhring, M.N. Monier, E. Kukk, J. Partanen, et al. 1996. The Tie receptor tyrosine kinase is expressed by human hematopoietic progenitor cells and by a subset of megakaryocytic cells. *Blood.* 6:2212–2220.
58. Takakura, N., X.-L. Huang, T. Naruse, I. Hamaguchi, D.J. Dumont, G.D. Yancopoulos, and T. Suda. 1998. Critical role of the TIE2 endothelial cell receptor in the development of definitive hematopoiesis. *Immunity.* 9:677–686.
59. Schwarze, S.R., A. Ho, A. Vocero-Akbani, and S.F. Dowdy. 1999. In vivo protein transduction: delivery of a biologically active protein into the mouse. *Science.* 285:1569–1572.
60. Hardy, R.R., C.E. Carmack, S.A. Shinton, J.D. Kemp, and K. Hayakawa. 1991. Resolution and characterization of pro-B and pre–pro-B cell stages in normal mouse bone marrow. *J. Exp. Med.* 5:1213–1225.
61. Sligh, J.E., Jr., C.M. Ballantyne, S.S. Rich, H.K. Hawkins, C.W. Smith, A. Bradley, and A.L. Beaudet. 1993. Inflammatory and immune responses are impaired in mice deficient in intercellular adhesion molecule 1. *Proc. Natl. Acad. Sci. USA.* 18:8529–8533.
62. Xu, H., J.A. Gonzalo, Y. St. Pierre, I.R. Williams, T.S. Kupper, R.S. Cotran, T.A. Springer, and J.-C. Gutierrez-Ramos. 1994. Leukocytosis and resistance to septic shock in intracellular adhesion molecule 1–deficient mice. *J. Exp. Med.* 180: 95–109.
63. Andrew, D.P., J.P. Spellberg, H. Takimoto, R. Schmits, T.W. Mak, and M.M. Zukowski. 1998. Transendothelial migration and trafficking of leukocytes in LFA-1-deficient mice. *Eur. J. Immunol.* 28:1959–1969.
64. Leuker, C., M. Labow, W. Müller, and N. Wagner. 2001. Neonatally induced inactivation of the vascular cell adhesion molecule 1 gene impairs B cell localization and T cell–dependent humoral immune response. *J. Exp. Med.* 193:755–767.
65. Koopman, G., R.M. Keehnen, E. Lindhout, W. Newman, Y. Shimizu, G.A. van Seventer, C. de Groot, and S.T. Pals. 1994. Adhesion through the LFA-1 (CD11α/CD18)-ICAM-1 (CD54) and the VLA-4 (CD49d)-VCAM-1 (CD106) pathways prevents apoptosis of germinal center B cells. *J. Immunol.* 8:3760–3767.

66. Skibinski, G., A. Skibinski, G.D. Stewart, and K. James. 1998. Enhancement of terminal B lymphocyte differentiation in vitro by fibroblast-like stromal cells from human spleen. *Eur. J. Immunol.* 28:3940–3948.
67. Merville, P., J. Dechanet, A. Desmouliere, I. Durand, O. de Bouteiller, P. Garrone, J. Banchereau, and Y.J. Liu. 1996. Bcl-2^+ tonsillar plasma cells are rescued from apoptosis by bone marrow fibroblasts. *J. Exp. Med.* 1:227–236.
68. Tripp, R.A., D.J. Topham, S.R. Watson, and P.C. Doherty. 1997. Bone marrow can function as a lymphoid organ during a primary immune response under conditions of disrupted lymphocyte trafficking. *J. Immunol.* 8:3716–3720.
69. Gaidano, G., and R. Dalla-Favera. 1997. Lymphomas. *In* Cancer: Principles and Practice of Oncology. V.T. DeVita, Jr., S. Hellman, and S.A. Rosenberg, editors. Lippincott-Raven Publishers, Philadelphia. 2131–2283.
70. Drew, M., H.F. Barker, J. Ball, C. Pearson, G. Cook, and I. Franklin. 1996. Very late antigen (VLA) expression by normal and neoplastic human plasma cells, including an assessment of antibodies submitted to the Vth International Workshop on Leucocyte Differentiation Antigens using human myeloma cell lines. *Leuk. Res.* 7:619–624.
71. Bataille, R., and J.L. Harousseau. 1997. Multiple myeloma. *N. Engl. J. Med.* 23:1657–1664.
72. Mundy, G.R. 1998. Myeloma bone disease. *Eur. J. Cancer.* 2:246–251.
73. Okada, T., R.G. Hawley, M. Kodaka, and H. Okuno. 1999. Significance of VLA-4-VCAM-1 interaction and CD44 for transendothelial invasion in a bone marrow metastatic myeloma model. *Clin. Exp. Metastasis.* 7:623–629.
74. Michigami, T., N. Shimizu, P.J. Williams, M. Niewolna, S.L. Dallas, G.R. Mundy, and T. Yoneda. 2000. Cell-cell contact between marrow stromal cells and myeloma cells via VCAM-1 and $\alpha4\beta1$-integrin enhances production of osteoclast-stimulating activity. *Blood.* 5:1953–1960.